

Sensory and Motor Systems

Divergent Modulation of Nociception by Glutamatergic and GABAergic Neuronal Subpopulations in the Periaqueductal Gray

 Vijay K. Samineni,^{1,5} Jose G. Grajales-Reyes,^{1,2,3,5} Bryan A. Copits,^{1,5} Daniel E. O'Brien,^{1,3,5} Sarah L. Trigg,^{1,5} Adrian M. Gomez,¹  Michael R. Bruchas,^{1,4,5} and  Robert W. Gereau IV^{1,5}

DOI:<http://dx.doi.org/10.1523/ENEURO.0129-16.2017>

¹Washington University Pain Center and Department of Anesthesiology, Washington University School of Medicine, St. Louis, MO 63110, ²Medical Scientist Training Program, Washington University School of Medicine, St. Louis, MO 63110, ³Division of Biomedical and Biological Sciences Graduate Program in Neuroscience, Washington University School of Medicine, St. Louis, MO 63110, ⁴Department of Neuroscience, Washington University School of Medicine, St. Louis, MO 63110, and ⁵Washington University School of Medicine, St. Louis, MO 63110

Abstract

The ventrolateral periaqueductal gray (vlPAG) constitutes a major descending pain modulatory system and is a crucial site for opioid-induced analgesia. A number of previous studies have demonstrated that glutamate and GABA play critical opposing roles in nociceptive processing in the vlPAG. It has been suggested that glutamatergic neurotransmission exerts antinociceptive effects, whereas GABAergic neurotransmission exerts pronociceptive effects on pain transmission, through descending pathways. The inability to exclusively manipulate subpopulations of neurons in the PAG has prevented direct testing of this hypothesis. Here, we demonstrate the different contributions of genetically defined glutamatergic and GABAergic vlPAG neurons in nociceptive processing by employing cell type-specific chemogenetic approaches in mice. Global chemogenetic manipulation of vlPAG neuronal activity suggests that vlPAG neural circuits exert tonic suppression of nociception, consistent with previous pharmacological and electrophysiological studies. However, selective modulation of GABAergic or glutamatergic neurons demonstrates an inverse regulation of nociceptive behaviors by these cell populations. Selective chemogenetic activation of glutamatergic neurons, or inhibition of GABAergic neurons, in vlPAG suppresses nociception. In contrast, inhibition of glutamatergic neurons, or activation of GABAergic neurons, in vlPAG facilitates nociception. Our findings provide direct experimental support for a model in which excitatory and inhibitory neurons in the PAG bidirectionally modulate nociception.

Key words: chemogenetics; Descending modulation; DREADDs; PAG; pain; RVM

Significance Statement

The periaqueductal gray (PAG) is a midbrain region critical for the modulation of pain. However, the roles played by the distinct cell types within the PAG in nociceptive processing are poorly understood. This work addresses the divergent roles of glutamatergic and GABAergic PAG neuronal subpopulations in nociceptive processing. We demonstrate that activation of glutamatergic neurons or inhibition of GABAergic neurons suppresses nociception. However, inhibition of glutamatergic neuronal activity or activation of GABAergic neuronal activity potentiates nociception. This report identifies distinct roles for these neuronal populations in modulating nociceptive processing.

Introduction

The periaqueductal gray (PAG), an evolutionarily conserved neurosubstrate in the midbrain, regulates a wide of

complex behaviors, including pain (Basbaum and Fields, 1978; Graeff et al., 1993; Behbehani, 1995; Bandler and Keay, 1996; Holstege, 2014; Tovote et al., 2016;

Received May 20, 2016; accepted March 3, 2017; First published March 17, 2017.

The authors declare no competing financial interests.

Author contributions: V.K.S. and R.W.G. designed research; V.K.S., B.A.C., J.G.G.R., and D.E.O. performed research; M.R.B. contributed unpublished reagents/analytic tools; V.K.S., J.G.G.R., B.A.C., R.W.G., A.M.G.,

Watson et al., 2016). The ventrolateral PAG (vlPAG) is a major site of endogenous opioid-induced pain suppression, and electrical stimulation of the vlPAG produces profound analgesia (Reynolds, 1969; Liebeskind et al., 1973; Mayer and Liebeskind, 1974; Hosobuchi et al., 1977; Baskin et al., 1986; Fields, 2004). The robust modulatory role of the vlPAG on spinal nociceptive processing is mediated by descending projections from the vlPAG via the rostral ventromedial medulla (RVM; Liebeskind et al., 1973; Basbaum and Fields, 1979; Bennett and Mayer, 1979; Hayes et al., 1979; Beitz et al., 1983; Duggan and Morton, 1983; Watkins et al., 1983; Morton et al., 1984; Moreau and Fields, 1986; Morgan et al., 1989; Urban and Smith, 1994; Pertovaara et al., 1996; Waters and Lumb, 1997; Antal and Odeh, 1998; Budai and Fields, 1998; Odeh and Antal, 2001; Maione et al., 2006; Waters and Lumb, 2008).

Previous studies have suggested that the vlPAG has a bidirectional role in the modulation of nociception. Non-specific activation of vlPAG neurons produces analgesia, whereas inhibition of vlPAG produces hyperalgesia to noxious stimulation (Reynolds, 1969; Liebeskind et al., 1973; Moreau and Fields, 1986; Depaulis et al., 1987; Siegfried and de Souza, 1989). It is tempting to speculate that output from the vlPAG has a purely analgesic action. However, the vlPAG comprises diverse subpopulations of neurons with distinct neurochemical properties that regulate excitatory and inhibitory neurotransmission (Behbehani and Fields, 1979; Moss and Basbaum, 1983; Moss et al., 1983; Moreau and Fields, 1986; Behbehani et al., 1990; Behbehani, 1995; Vaughan et al., 1997; Hahm et al., 2011; Ho et al., 2013). Microinjection of glutamate receptor agonists or GABA antagonists into the vlPAG leads to global activation of neurons and produces antinociceptive effects to noxious stimuli (Moreau and Fields, 1986; Ness and Gebhart, 1987; Carstens et al., 1988; Jacquet, 1988; Jones and Gebhart, 1988; Jensen and Yaksh, 1989; Sandkühler et al., 1989; Carstens et al., 1990; Budai and Fields, 1998; Morgan et al., 2003). In contrast, microinjecting glutamatergic antagonists or GABA agonists, presumably leading to global suppression of neural activity in the vlPAG, produces hyperalgesia (Moreau and Fields, 1986; Depaulis et al., 1987; Siegfried and de Souza, 1989; Behbehani et al., 1990). These studies suggest that in the context of a noxious stimulus, GABAergic neurotransmis-

sion in the vlPAG is pronociceptive, although the source of the GABAergic inputs to the vlPAG cannot be determined (Reichling and Basbaum, 1990a, 1990b). Collectively, a large number of prior studies suggest that glutamatergic and GABAergic neurons within the vlPAG play critical and complex roles in processing nociception (Behbehani and Fields, 1979; Moreau and Fields, 1986; Millan et al., 1987; Sandkühler et al., 1989; Siegfried and de Souza, 1989; Vaughan et al., 1997). Based on these studies, the vlPAG GABA disinhibition hypothesis has been proposed (Basbaum and Fields, 1978; Fields, 2004; Lau and Vaughan, 2014). In this hypothesis, GABAergic interneurons exert tonic inhibition over vlPAG glutamatergic neurons, which are thought to be output neurons that project to the RVM to facilitate the descending inhibition of nociception (Vaughan et al., 1997; Budai and Fields, 1998; Wang and Wessendorf, 2002; Maione et al., 2006; Starowicz et al., 2007; Heinricher et al., 2009; Park et al., 2010; Tovote et al., 2016). Despite the wealth of evidence supporting this model, the distinct roles of GABAergic and glutamatergic neuronal populations in descending vlPAG pain modulation have not been directly investigated. In this study, we use cell type-specific chemogenetic manipulations of neuronal activity in the vlPAG to test the hypothesis that GABAergic neurons are pronociceptive and glutamatergic neurons are antinociceptive.

Materials and Methods

Animals

All experiments were conducted in accordance with the National Institutes of Health guidelines and with approval from the Animal Care and Use Committee of Washington University School of Medicine. Male, 8- to 12-week-old, heterozygous *Slc32a1^{tm2Lowl}* (Vgat-ires-Cre, selectively targets Vgat⁺ GABAergic inhibitory neurons), *Slc17a6^{tm2Lowl}* (Vglut2-ires-Cre, selectively targets Vglut2⁺ glutamatergic excitatory neurons), and C57BL/6J mice were used (Vong et al., 2011). Mice were purchased from Jackson Laboratories (C57BL/6J, Vgat Cre, stock number 016962 and Vglut2 Cre stock number 016963) and colonies were established in our facilities. Experimenters were blind to treatment and genotype.

Viral constructs and surgery

Adeno-associated viruses (AAV8) were used to achieve Cre-independent chemogenetic vector expression: hM3Dq-mCherry (rAAV8/hSyn-hM3Dq-mCherry; 3.2×10^{12} particles/ml), hM4Di-mCherry (rAAV8/hSyn-hM4Di-mCherry; 2×10^{12} particles/ml), and control eGFP (rAAV8/hSyn-eGFP; 8×10^{12} particles/ml). Adeno-associated viruses (AAV5) were used to achieve Cre-dependent vector expression: hM3Dq-mCherry (rAAV5/hSyn-DIO-hM3Dq-mCherry; 6×10^{12} particles/ml), hM4Di-mCherry (rAAV5/hSyn-DIO-hM4Di-mCherry; 6×10^{12} particles/ml), and control eGFP (rAAV5/hSyn-DIO-eGFP; 3.4×10^{12} particles/ml). All viral vectors were acquired from the University of North Carolina Vector Core Facility. Before surgery, mice were anesthetized with isoflurane and secured in a stereotactic frame (David Kopf Instruments). A small midline dorsal incision was per-

and S.L.T. analyzed data; V.K.S. and R.W.G. wrote the paper.

³ This work was funded by the NIH Director's Transformative Research Award TR01 NS081707 (to R.W.G. and M.R.B.), the NINDS R01NS048602 (to R.W.G.), Urology Care Foundation Research Scholars Program and Kailash Kedia Research Scholar Award to V.K.S., the NIGMS Training Grant T32 GM108539 (to B.A.C.), and the Medical Scientist Training Program (MSTP) Grant T32GM07200 (to J.G.G.R.).

Correspondence should be addressed to Robert W. Gereau IV, Department of Anesthesiology, Washington University School of Medicine, 660 S. Euclid Avenue, Campus Box 8054, St. Louis, MO 63110, E-mail: gereaur@wustl.edu.

DOI: <http://dx.doi.org/10.1523/ENEURO.0129-16.2017>

Copyright © 2017 Samineni et al.

This is an open-access article distributed under the terms of the Creative Commons Attribution 4.0 International license, which permits unrestricted use, distribution and reproduction in any medium provided that the original work is properly attributed.

formed to expose the skull and bilateral viral injections were performed using the following coordinates: vIPAG, -4.8 – -4.9 mm from bregma, ± 0.3 – 0.4 mm lateral from midline, and 2.7 – 2.9 mm ventral to skull. Injections of 150 nL of the desired viral vectors into the vIPAG were performed at a rate of 100 nl per 60 s.

Chemogenetic manipulation

Three weeks after viral injections, mice were injected intraperitoneally with clozapine N-oxide (CNO, BML-NS105 from Enzo life sciences) 60 min before beginning behavioral assessment, and data were collected between the second and third hour after injection. All baselines for thermal and mechanical sensitivity were recorded two weeks after the viral injections and one week before the CNO administration. The doses of CNO were chosen based on preliminary pilot experiments designed to determine the minimal dose needed to activate designer receptor exclusively activated by designer drugs (DREADD) receptors in the vIPAG of C57BL/6J mice, Vgat-ires-Cre and Vglut2-ires-Cre mice. We assessed the response of these different mouse lines to various doses of CNO to identify the minimal doses required to activate DREADDs (data not shown). In non-Cre-dependent studies, we administered 1 mg/kg CNO for both hM3Dq activation and hM4Di inhibition. In Vgat Cre mice, we administered 3 mg/kg CNO for both hM3Dq activation and hM4Di inhibition. In Vglut2 Cre mice, we administered 2 mg/kg CNO for both hM3Dq activation and hM4Di inhibition.

Pain behavior assessment

To evaluate nociception, mechanical withdrawal thresholds and thermal withdrawal latencies were assayed. Mice were tested for baseline responses to mechanical and thermal stimuli, as previously described (O'Brien et al., 2013). For the assessment of mechanical withdrawal threshold, von Frey filaments (North Coast Medical) were applied bilaterally to the hind paws of the mice using the up-down method. Two to three trials were performed on each hind paw for each mouse. The average 50% withdrawal threshold was calculated for each paw individually and then averaged to obtain a threshold value for each mouse. The Hargreaves test was performed to evaluate heat sensitivity thresholds, measuring latency of withdrawal to a radiant heat source (IITC Life Science, Model 390). We applied the radiant heat source bilaterally to the hind paw and measured the latency to evoke a withdrawal. Three to five replicates were acquired per hind paw per mouse, and values for both paws were averaged.

Electrophysiology

To determine the functional effects of chemogenetic manipulations in vIPAG neurons, we performed targeted whole-cell patch-clamp recordings in acute coronal slices from both Vgat- and Vglut2-Cre mice expressing either hM3Dq or hM4Di receptors. Mice used for electrophysiology and behavioral studies were between 8 and 12 weeks of age. Three weeks after viral infection of vIPAG neurons, coronal slices containing the vIPAG were prepared as previously described (Siuda et al., 2015). GABAergic and glutamatergic neurons in the vIPAG were

visualized through a $40\times$ objective using IR-differential interference contrast (DIC) microscopy on an Olympus BX51 microscope, and mCherry+ cells were identified using epifluorescent illumination with a green LED (530 nm; Thorlabs), coupled to the back fluorescent port of the microscope. Whole-cell recordings of vIPAG GABAergic and glutamatergic neurons expressing hM3Dq-mCherry and hM4Di-mCherry were performed using a Heka EPC 10 amplifier (Heka) with Patchmaster software (Heka). Following stable 5 -min whole-cell recordings (baseline), the direct effects of either hM3Dq or hM4Di receptor expression on cellular excitability was isolated by blocking AMPA/KARs (10 μ M NBQX, Abcam), NMDARs (50 μ M D-APV, Abcam), GABA_ARs (100 μ M picrotoxin, Abcam), and GABA_BRs (50 μ M baclofen, Abcam). aCSF solution containing 10 μ M CNO added to the antagonist cocktail above was bath applied to the brain slice.

Immunohistochemistry

To perform histologic confirmation of virus expression and injection sites, C57, Vgat Cre, and Vglut2 Cre mice expressing hM3Dq-mCherry, hM4Di-mCherry, and EGFP virus were deeply anesthetized with ketamine/xylazine cocktail at the end of every experiment and then perfused with 20 ml of PBS and 20 ml of a 4% paraformaldehyde PBS solution (PFA). Brains were removed, postfixed in 4% PFA overnight at 4° , and then immersed in 30% sucrose for cryoprotection. Using a cryostat, 30 - μ m tissue sections were collected and stored in PBS, containing 0.4% sodium azide, at 4° . After washing the sections in PBS $1\times$, we incubated the tissues in blocking solution containing 5% normal goat serum and 0.2% Triton X-100 PBS solution for 1 h at room temperature. Primary antibodies against mCherry (Mouse, Clontech 632392; $1:500$) and GFP (rabbit polyclonal, Life Technologies A11122, $1:500$) were diluted in blocking solution and incubated overnight at 4° . After three 10 -min washes, tissues were incubated for 1 h at room temperature with secondary antibodies [Life Technologies: Alexa Fluor 488 donkey anti rabbit IgG ($1:300$); Alexa Fluor 488 goat anti rabbit ($1:300$); Alexa Fluor 555 goat anti mouse ($1:300$); and Neurotrace ($435/455$ nm, $1:500$)]. Sections were mounted with Vectashield (H-1400) hard mounting media and imaged on a Nikon Eclipse 80i epifluorescence microscope.

Fluorescence in situ hybridization (FISH)

Following rapid decapitation of mice, brains were flash frozen in -50° C 2-methylbutane and stored at -80° C for further processing. Coronal sections containing the PAG, corresponding to the injection coordinates used in the behavioral experiments, were cut at 20 μ m at -20° C and thaw-mounted onto Super Frost Plus slides (Fisher). Slides were stored at -80° C until further processing. FISH was performed according to the RNAScope 2.0 Fluorescent Multiple Kit User Manual for Fresh Frozen Tissue (Advanced Cell Diagnostics) as described previously (Wang et al., 2012). Slides containing PAG coronal brain sections were fixed in 4% PFA, dehydrated, and pre-treated with protease IV solution for 30 min. Sections were then incubated with target probes for mouse Vglut2 (*slc17a6*, accession number NM_080853.3, probe region

1986-2998), *Vgat* (*slc32a1*, accession number NM_009508.2, probe region 894-2037), and Cre (accession number KC845567.1, probe region 1058-2032). All target probes consisted of 20 double Z oligonucleotides and were obtained from Advanced Cell Diagnostics. Following probe hybridization, sections underwent a series of probe signal amplification steps (AMP1-4) followed by incubation of fluorescent probes (Alexa Fluor 488, Atto 550, Atto 647), designed to target the specified channel associated with the probes. Slides were counterstained with 4',6-diamidino-2-phenylindole (DAPI; RNAScope), and coverslips were mounted with Vectashield Hard Set mounting medium (Vector Laboratories). Images were obtained on a Leica TCS SPE confocal microscope (Leica), and Application Suite Advanced Fluorescence (LAS AF) software was used for analyses.

Statistics

Throughout the study, researchers were blinded to all experimental conditions. At least two to three replicate measurements were performed and averaged in all behavioral assays. The studies were designed to compare behavioral readouts following CNO to baseline values before CNO administration. This was done using paired *t* tests to account for interindividual variability among mice across different cohorts. The control eGFP group was included throughout our study to determine whether CNO administration or DREADD expression had off-target effects in the behaviors that we tested. All datasets were evaluated for normality using the D'Agostino and Pearson omnibus normality test. A parametric test was used only when normality was confirmed. If normality could not be confirmed, the nonparametric Wilcoxon matched pairs test was used.

Results

Global chemogenetic manipulation of vIPAG activity suggests bidirectional modulation of nociceptive behaviors

We used a chemogenetic approach to investigate whether selectively manipulating activity of resident neurons in the vIPAG can modulate different nociceptive modalities. DREADDs exploit selective expression of mutated muscarinic receptors that are responsive to an exogenously administered, normally inert ligand, CNO (Rogan and Roth, 2011). Adeno-associated virus type 8 (AAV8), carrying neuron-specific stimulatory (hM3Dq) or inhibitory (hM4Di) DREADD fused with mCherry, was microinjected bilaterally into the vIPAG (Fig. 1A). Robust expression of DREADDs, restricted to the vIPAG, was observed three weeks after AAV8/hSyn-hM3Dq-mCherry (Fig. 1B) or AAV8/hSyn-hM4Di-mCherry injection (Fig. 1C). In mice expressing the stimulatory DREADD (hM3Dq) in vIPAG neurons, CNO (1 mg/kg, i.p.) injection resulted in a significant increase in paw withdrawal latencies (PWLs) to thermal stimulation compared with baseline PWLs before CNO administration but did not alter paw withdrawal thresholds (PWTs) to mechanical stimuli compared with baseline PWTs before CNO administration (Fig. 1E; $t_{(10)} = 3.674$, $**p = 0.0043$, $n = 11$; Fig. 1H; $t_{(10)} = 0.3489$, $p =$

0.73, $n = 11$). On the other hand, in mice expressing the inhibitory DREADD (hM4Di) in vIPAG neurons, CNO (1 mg/kg, i.p.) injection resulted in a significant decrease in PWLs and PWTs compared with baseline (Fig. 1F; $t_{(11)} = 6.693$, $***p < 0.0001$, $n = 12$; Fig. 1I; $*p < 0.05$, $n = 11$), indicating development of thermal and mechanical hypersensitivity. To confirm that CNO administration did not have any off-target effects on PWLs and PWTs, control mice expressing eGFP were administered CNO (1 mg/kg), which had no effect on PWLs or PWTs when compared with baseline (Fig. 1D; $t_{(11)} = 0.2572$, $p = 0.80$, $n = 12$; Fig. 1G, $t_{(8)} = 0.2945$, $p = 0.77$, $n = 9$). Taken together, these findings demonstrate that globally activating vIPAG neurons attenuates nociception, while inhibiting them potentiates nociception, consistent with prior studies using pharmacologic activation or inhibition of the vIPAG neurons (Moreau and Fields, 1986; Carstens et al., 1988; Jones and Gebhart, 1988; Jensen and Yaksh, 1989; Siegfried and de Souza, 1989; Behbehani et al., 1990; Carstens et al., 1990; Vaughan et al., 1997; Budai and Fields, 1998; Morgan et al., 2003).

The role of vIPAG GABAergic and glutamatergic neuronal populations in nociceptive processing

The vIPAG is comprised of both inhibitory GABAergic and excitatory glutamatergic neurons, and we hypothesized that these neuronal populations differentially regulate nociceptive processing. Double-label RNA-FISH in the vIPAG of c57-mice revealed that GABAergic neurons (*Vgat* transcripts) and glutamatergic neurons (*Vglut2* transcripts) show no overlap in expression in the PAG and, thus, are distinct populations (Fig. 2A,B). To selectively test the functional contributions of vIPAG GABAergic and glutamatergic neurons in modulating nociceptive behaviors, we used *Vgat*-ires-Cre and *Vglut2*-IRES-Cre mice to target and manipulate the activity of GABAergic and glutamatergic neurons, respectively. To determine the specificity of Cre in targeting *Vgat*⁺ neurons in *Vgat*-IRES-Cre mice or in targeting *Vglut2*⁺ neurons in the *Vglut2*-IRES-Cre mice, we performed RNA-FISH using probes for *Vgat*, *Vglut*, and Cre in vIPAG slices obtained from *Vgat* Cre and *Vglut2* Cre mice. We observed $79 \pm 4.1\%$ of *Vglut2*⁺ transcripts in the vIPAG colabel with *Vglut2* Cre-expressing neurons, and $97.5 \pm 2.5\%$ *Vglut2* Cre-expressing neurons in the vIPAG colabel with *Vglut2*⁺ transcripts (Fig. 2C,E-J). We also observed $92 \pm 4.5\%$ of *Vgat*⁺ transcripts in the vIPAG colabel with *Vgat* Cre-expressing neurons, and $95.5 \pm 4.2\%$ *Vgat* Cre-expressing neurons in the vIPAG colabel with *Vgat*⁺ transcripts (Fig. 2D,K-P). Our double-label RNA-FISH studies revealed that *Vgat* and *Vglut2* Cre mice faithfully label vIPAG GABAergic and *Vglut2*⁺ glutamatergic neuronal populations, as described previously for other brain regions (Vong et al., 2011).

To selectively test the functional contributions of vIPAG GABAergic and glutamatergic neurons in modulating nociceptive behaviors, we used Cre-dependent DREADD expression in *Vgat*-ires-Cre and *Vglut2*-ires-Cre mice to target GABAergic and glutamatergic neurons, respectively. Virus carrying Cre-dependent stimulatory (hM3Dq) or inhibitory (hM4Di) DREADDs fused with mCherry were

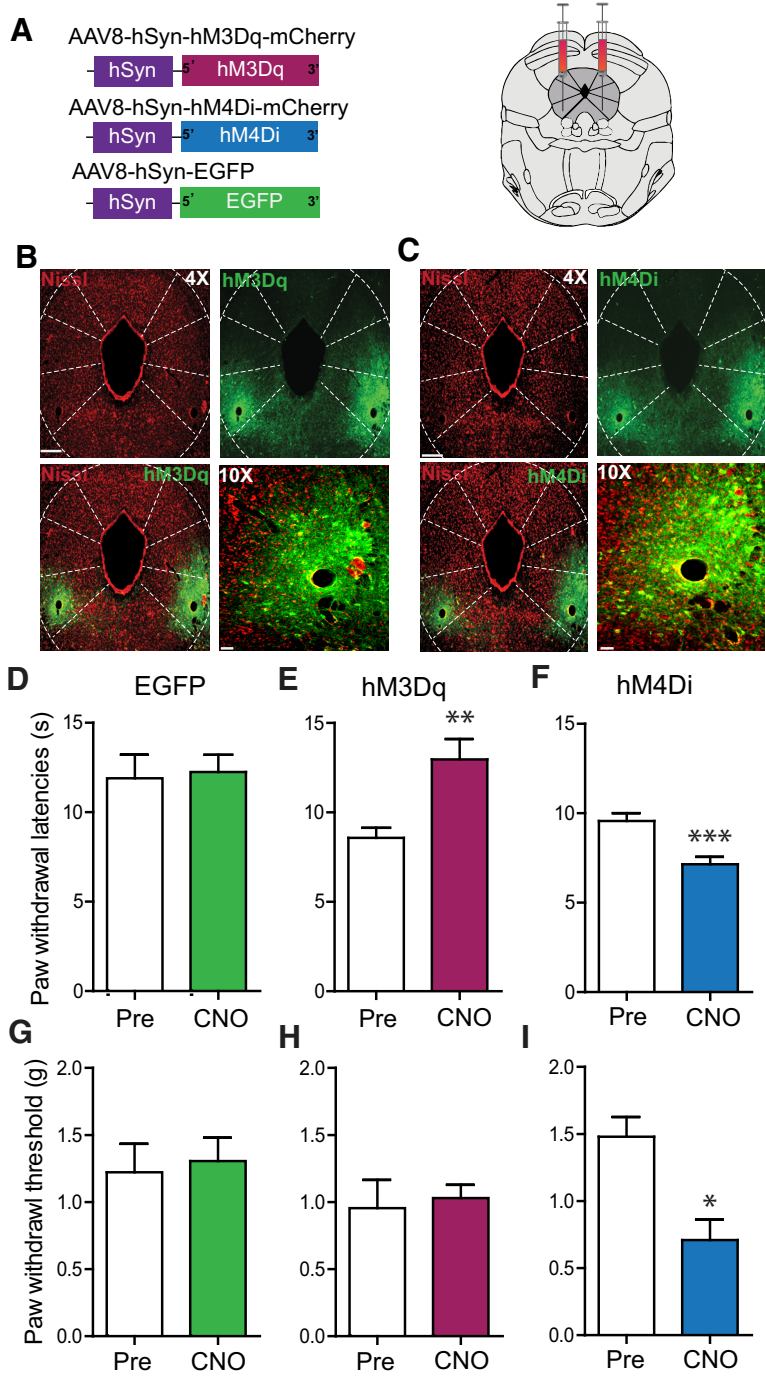


Figure 1. Global chemogenetic manipulation of vPAG activity suggests parallel bidirectional modulation of nociceptive behaviors. **A**, Constructs used in viral targeting of AAV8 hm3Dq-mCherry, AAV8 hm4Di-mCherry and AAV8-EGFP via bilateral injections into the vPAG. **B**, **C**, Representative images of coronal sections containing vPAG demonstrating restricted viral expression following microinjection of the AAV8 hm3Dq (**B**) and hm4Di (**C**) into the vPAG. **D**, **G**, Relative to pretreatment baseline values, CNO (1 mg/kg, i.p.) did not have any significant effects on PWLs in mice expressing the control EGFP construct. **E**, **H**, CNO (1 mg/kg, i.p.) administration in hm3Dq-injected mice resulted in a significant increase in PWLs but not in PWTs. **F**, **I**, CNO (1 mg/kg, i.p.) administration in hm4Di-injected mice resulted in a significant decrease in PWLs and PWTs. * $p < 0.05$, ** $p < 0.005$, *** $p < 0.0001$. Scale bars, 300 and 35 μm , 4 \times and 10 \times , respectively.

injected into the vPAG of Vgat-Cre mice or Vglut2-Cre mice. Three weeks after DREADD injection, we prepared acute coronal slices of the vPAG from Vgat-Cre and Vglut2-Cre mice and targeted mCherry⁺ neurons in vPAG for whole-

cell recordings (Fig. 3A). hm3Dq-expressing vPAG neurons were held at hyperpolarized membrane potentials, and a brief bath application of 10 μM CNO caused a transient depolarization and robust action potential firing in both Vgat

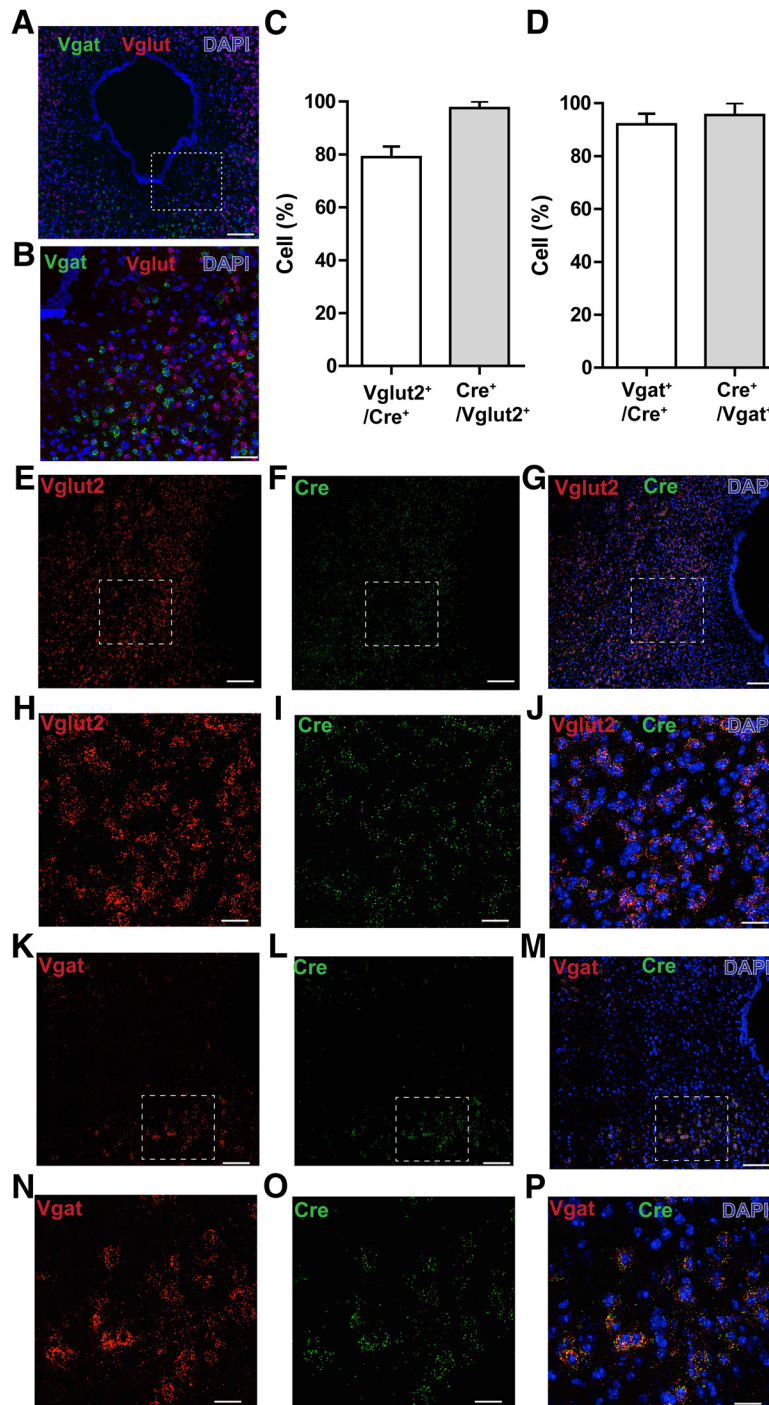


Figure 2. RNA-FISH demonstrates segregation of vPAG GABAergic and glutamatergic neurons and specificity of Cre in targeting *Vgat*⁺ neurons in the *Vgat*-IRES-Cre mice or *Vglut2*⁺ neurons in the *Vglut2*-IRES-Cre mice. **A**, Double RNA-FISH for *Vgat* (green) and *Vglut2* (red) shows that GABAergic and glutamatergic neurons in the PAG are nonoverlapping populations. Scale bar, 200 μ m. Counterstaining (blue) is DAPI. **B**, High-magnification image showing no colocalization of GABAergic and glutamatergic neurons in the PAG. Scale bar, 60 μ m. **C**, 79 \pm 4.1% of cells positive for *Vglut2* transcripts in the vPAG colabel with *Vglut2* Cre-expressing neurons, and 97.5 \pm 2.5% of *Vglut2* Cre-expressing neurons in the vPAG colabel with *Vglut2*⁺ transcripts (*N* = 2 mice). **D**, 92 \pm 4.5% of cells positive for *Vgat* transcripts in the vPAG colabel with *Vgat* Cre-expressing neurons, and 95.5 \pm 4.2% of *Vgat* Cre-expressing neurons in the vPAG colabel with *Vgat*⁺ transcripts (*N* = 2 mice). **E–G**, Double RNA-FISH for *Vglut2* (red) and Cre (green) shows extensive colocalization of *Vglut2*⁺ transcripts with Cre-expressing neurons in the vPAG obtained from *Vglut2* Cre mice. Scale bar, 60 μ m. **H–J**, High-magnification image shows extensive colocalization of *Vglut2*⁺ transcripts with Cre-expressing neurons in the vPAG. Scale bar, 15 μ m. **K, M**, Double RNA-FISH for *Vgat* (red) and Cre (green) shows extensive colocalization of *Vgat*⁺ transcripts with Cre-expressing neurons in the vPAG obtained from *Vgat* Cre mice. Scale bar, 60 μ m. **N–P**, High-magnification image shows extensive colocalization of *Vgat*⁺ transcripts with Cre-expressing neurons in the vPAG. Scale bar, 15 μ m.

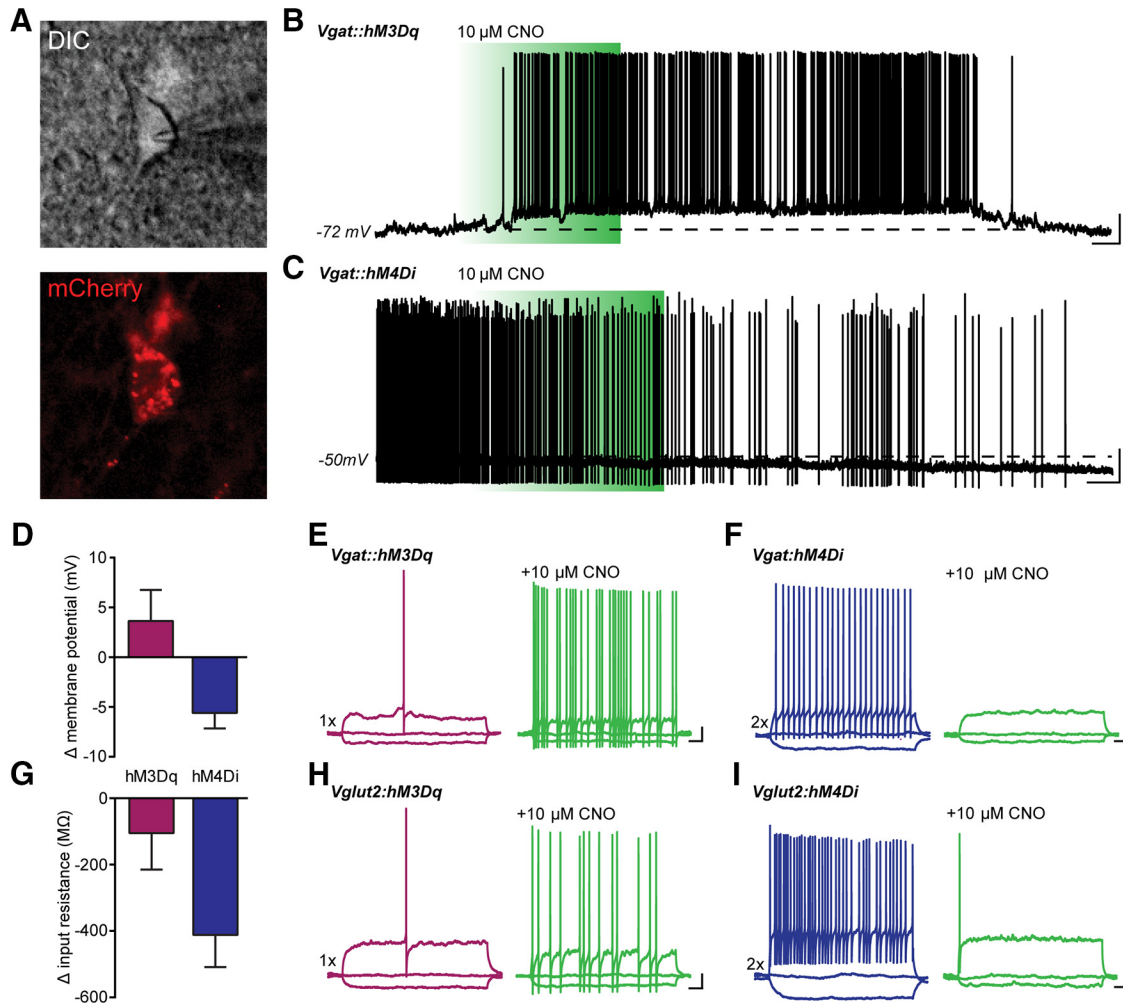


Figure 3. Functional characterization of G_q - and G_i -DREADDs in vPAG neurons of *Vgat*-Cre and *Vglut2*-Cre mice. **A**, Infrared DIC image of vPAG *Vgat*⁺ neuron expressing hM4Di-mCherry. Images were acquired following CNO stimulation. **B**, Whole-cell current-clamp recording from an hM3Dq-expressing PAG neuron. Brief bath application of 10 μ M CNO caused a transient depolarization and robust action potential firing in *Vgat*⁺ and *Vglut*⁺ neurons. **C**, Voltage trace showing that bath perfusion with 10 μ M CNO caused prolonged membrane hyperpolarization and silencing of both *Vgat*⁺ and *Vglut*⁺ vPAG neurons. Dashed lines in **B** and **C** represent the membrane potential of the cells before application of CNO. **D**, **G**, Quantification of the CNO effects on membrane potential and input resistance in grouped *Vgat*⁺ and *Vglut2*⁺ neurons ($N = 8$ for *Vgat*⁺ and *Vglut2*⁺ neurons). **E–I**, Voltage traces showing responses to a hyperpolarizing current of -20 pA and a depolarizing current injection of either 1 \times rheobase (purple traces) or 2 \times rheobase (blue traces) in both *Vgat*⁺ (**E**, **H**) and *Vglut2*⁺ (**F**, **I**) neurons. In hM3Dq-expressing neurons, bath application of CNO elicited increased action potential firing in response to the same stimulus (**E**, **H**, green traces). In hM4Di⁺ neurons, CNO perfusion decreased neuronal excitability to suprathreshold stimuli. **B**, **C**, Scale bars, 20 mV and 10 s; **E–I**, Scale bars, 10 mV and 100 ms. All values are mean \pm SEM.

and *Vglut2* neurons (Fig. 3B). To test the effects of G_i -coupled inhibition with hM4Di, we monitored neuronal activity while holding cells with a depolarizing current injection, which elicited persistent action potential firing in both *Vgat* and *Vglut2* neurons. Bath perfusion with 10 μ M CNO resulted in prolonged membrane hyperpolarization and decreased firing of both cell types (Fig. 3C). Quantification of hM3Dq-expressing neurons showed that CNO depolarized neurons by an average of 3.6 mV and caused a small decrease in the input resistance (Fig. 3D,G). In contrast, activation of hM4Di hyperpolarized neurons by an average of 5.6 mV, and substantially reduced input resistance, consistent with CNO-induced G_i -coupling to inwardly rectifying

K^+ channels (Stensson and Roth, 2014; Urban and Roth, 2015; Fig. 3D,G).

We also investigated how CNO modulates membrane excitability in response to depolarizing step current injections. In hM3Dq-expressing neurons, we observed a large increase in the number of action potentials elicited during a 1 \times rheobase current following CNO stimulation in slices from both *Vgat*- and *Vglut2*-Cre mice (Fig. 3E,H). Suprathreshold current injections of 2 \times rheobase elicited sustained high-frequency action potential firing in both neuronal subtypes (Fig. 3F,I, blue traces), and CNO application dramatically reduced membrane excitability to an identical suprathreshold stimulus in mice injected with

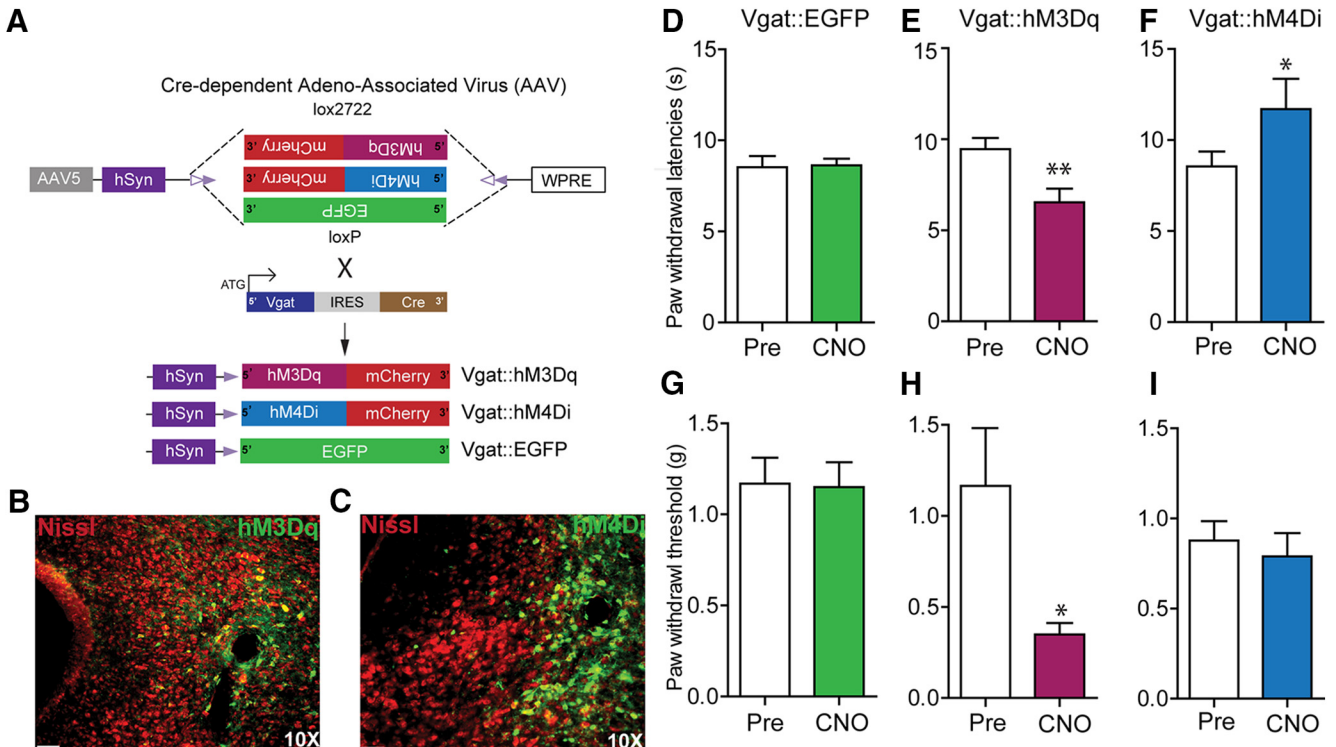


Figure 4. Chemogenetic manipulation of vPAG GABAergic neurons bidirectionally modulates nociceptive behaviors. **A**, Illustration showing viral targeting strategy of AAV5-hSyn-DIO-hM3Dq-mCherry, AAV5-hSyn-DIO-hM4Di-mCherry, and AAV5-hSyn-DIO-EGFP bilaterally injected into the vPAG of Vgat Cre mice. **B**, **C**, Representative images of coronal sections containing vPAG showing restricted viral expression following microinjection of AAV5-hSyn-DIO-hM3Dq (**B**) or AAV5-hSyn-DIO-hM4Di (**C**) into the vPAG of Vgat Cre mice. **E**, **H**, CNO (3 mg/kg, i.p.) administration resulted in a significant decrease in PWLs and PWTs in Vgat::hM3Dq mice. **F**, **I**, CNO administration resulted in a significant increase in PWLs but not in PWTs in Vgat::hM4Di mice. **D**, **G**, CNO had no significant effect on PWLs or PWTs in Vgat Cre mice expressing the control EGFP construct compared with baseline PWLs and PWTs before CNO administration. All values are mean \pm SEM. Student's *t* test; **p* < 0.05, ***p* < 0.005. Scale bars, 25 μ m.

hM4Di constructs (Fig. 3*F,I*, green traces). This confirmed that we are able to bi-directionally modulate GABAergic and glutamatergic neuron excitability in the vPAG using hM3Dq and hM4Di DREADDs, and led us to explore the contributions of these neuronal populations in nociceptive processing.

To assess how vPAG GABAergic neurons contribute to nociceptive processing, we introduced Cre-dependent viral constructs containing either hM3Dq or hM4Di fused to mCherry or control virus lacking the DREADDs (hSyn-DIO-eGFP) into the vPAG of Vgat-IRES-Cre mice (Fig. 4*A*). Three weeks after viral infection of vPAG neurons, restricted expression of the DREADD vectors was observed in neurons within the vPAG (Fig. 4*B,C*). CNO-dependent (3 mg/kg, i.p.) activation of vPAG GABAergic neurons via hM3Dq resulted in a significant decrease in PWLs to a noxious thermal stimulus (Fig. 4*E*; $t_{(8)} = 4.403$, $p = 0.0023$, $n = 9$) and PWTs to a mechanical stimulus (Fig. 4*H*; $p = 0.0469$, $n = 7$) compared with baseline. In contrast, CNO-induced (3 mg/kg, i.p.) inhibition of vPAG GABAergic neurons expressing hM4Di resulted in a significant increase in PWLs to noxious thermal stimulation compared with baseline (Fig. 4*F*, $t_{(13)} = 2.459$, $p = 0.0287$, $n = 14$) but did not have a significant effect on PWTs to mechanical stimuli compared with baseline (Fig. 4*I*; $t_{(11)} =$

0.5885, $p = 0.5681$, $n = 12$). CNO (3 mg/kg, i.p.) administration did not affect PWLs or PWTs in control mice expressing DIO-EGFP when compared with baseline (Fig. 4*D*; $t_{(9)} = 0.1837$, $p = 0.8584$, $n = 10$) and (Fig. 4*G*; $t_{(8)} = 0.2055$, $p = 0.8423$, $n = 9$). Taken together, these results demonstrate that activation of GABAergic vPAG neurons results in hypersensitivity to mechanical and noxious thermal stimuli, while inhibiting the activity of GABAergic vPAG neurons decreases sensitivity to noxious heat only.

To directly examine the role of vPAG glutamatergic neurons in nociceptive processing, Cre-dependent viral constructs carrying hM3Dq-mCherry, hM4Di-mCherry, or a control virus (hSyn-DIO-eGFP) were injected bilaterally into the vPAG of Vglut2-ires-Cre mice (Fig. 5*A*). Three weeks after injection, we observed robust DREADD expression restricted to the vPAG (Fig. 5*B,C*). Chemogenetic activation of vPAG Vglut2 neurons expressing hM3Dq with CNO (2 mg/kg, i.p.) significantly increased PWLs to thermal stimuli compared with baselines before CNO administration (Fig. 5*E*; $t_{(11)} = 2.375$, $p = 0.0368$, $n = 12$) but did not significantly alter PWTs to mechanical stimuli compared with baseline (Fig. 5*H*; $t_{(8)} = 0.8779$, $p = 0.405$, $n = 9$). To further examine the functional role of intrinsic activity of vPAG Vglut2 neurons, we administered CNO (2 mg/kg, i.p.) to inhibit vPAG Vglut2 neurons expressing hM4Di. This resulted in a significant decrease

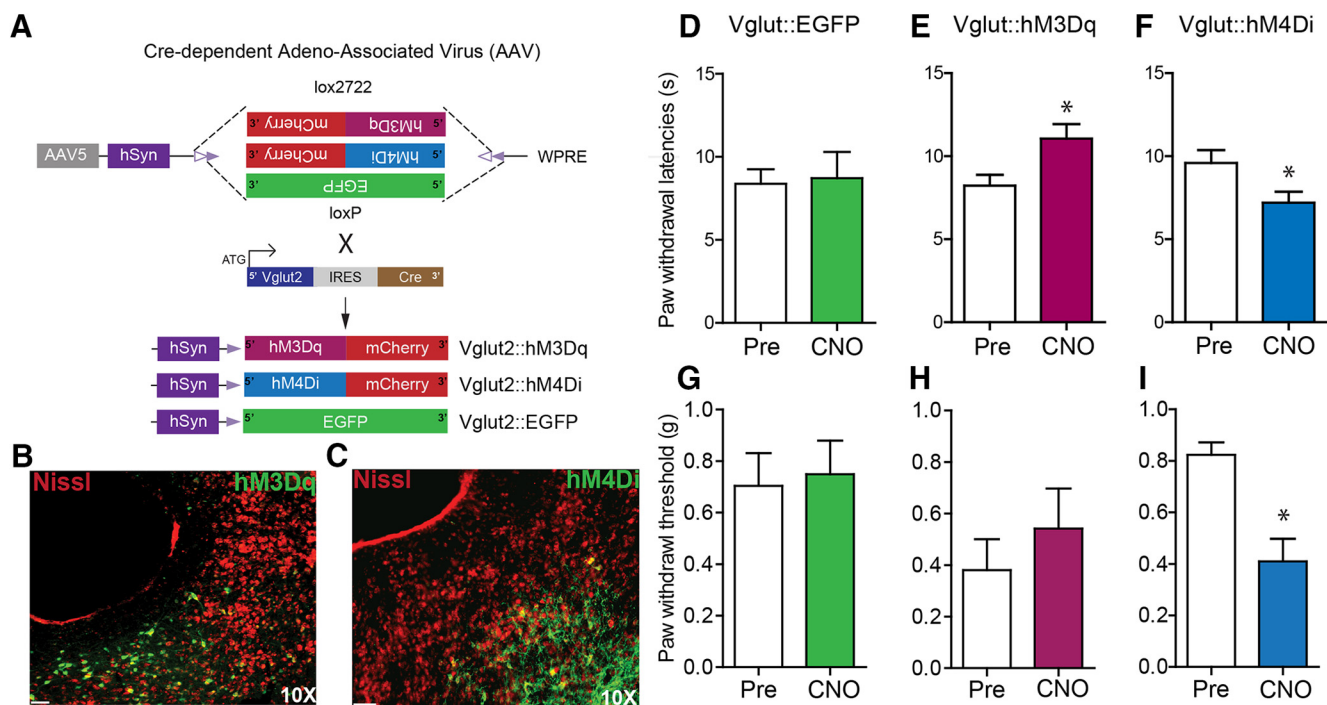


Figure 5. Chemogenetic modulation of vPAG glutamatergic neurons bidirectionally modulates nociceptive behaviors. **A**, Illustration showing the strategy for viral targeting of AAV5-hSyn-DIO-hM3Dq-mCherry, AAV5-hSyn-DIO-hM4Di-mCherry, and AAV5-hSyn-DIO-EGFP bilaterally injected into the vPAG of Vglut2 Cre mice. **B, C**, Representative images of a coronal sections containing vPAG showing restricted viral expression following microinjection of the AAV5-hSyn-DIO-hM3Dq-mCherry and AAV5-hSyn-DIO-hM4Di-mCherry into the vPAG of Vglut2 Cre mice. **E, H**, CNO (2 mg/kg, i.p.) administration resulted in a significant increase in PWLs but not on PWTs in Vglut2::hM3Dq mice. **F, I**, CNO (2 mg/kg, i.p.) administration resulted in a significant decrease in PWLs and PWTs in Vglut2::hM4Di mice. **D, G**, CNO had no significant effect on PWLs or PWTs in Vglut2 Cre mice expressing the control EGFP construct compared with baseline PWLs and PWTs before CNO administration. All values are mean \pm SEM, Student's *t* test; **p* < 0.05. Scale bars, 25 μ m.

in PWLs to a noxious heat stimulus compared with baseline (Fig. 5F; $n = 6$, paired *t* test, $p = 0.0313$) and a decrease in PWTs to a mechanical stimulus compared with baseline (Fig. 5I; $n = 6$, paired *t* test, $p = 0.0211$). Control virus-injected mice showed no alterations in PWTs or PWLs on CNO (2 mg/kg, i.p.) administration compared with baseline (Fig. 5D; $t_{(9)} = 0.2897$, $p = 0.7786$, $n = 10$; Fig. 5G, $p = 1$, $n = 6$). These results demonstrate that vPAG Vglut2 neurons exert tonic control over thermal and mechanical nociceptive processing.

Discussion

Here, we report that global chemogenetic activation of vPAG neurons attenuates thermal nociception while inhibiting vPAG neurons cause thermal and mechanical hypersensitivity. Using cell type-specific chemogenetic manipulations, we found that activating GABAergic, or inhibiting glutamatergic, neurons in vPAG, causes thermal and mechanical hypersensitivity. In contrast, inhibiting GABAergic or activating glutamatergic neurons attenuates thermal sensitivity but has no effect on mechanical sensitivity. The differential effects on thermal and mechanical sensitivity suggest that distinct circuit elements within the vPAG regulate these two sensory modalities. These results provide new insights into the functional role of GABAergic and glutamatergic neurons in the vPAG in the modulation of nociception.

The vPAG is known to be an essential component of neural pathways that mediate stimulation and stress-induced analgesia (Reynolds, 1969; Yeung et al., 1977; Jones and Gebhart, 1988; Morgan et al., 1989; Hohmann et al., 2005; Samineni et al., 2011). Consistent with these previous studies, we found that global chemogenetic activation of vPAG neurons produced antinociceptive effects. We also show that chemogenetic inhibition of vPAG neurons leads to nociceptive hypersensitivity, consistent with a bidirectional role of the vPAG in the modulation of nociception (Moreau and Fields, 1986; Depaulis et al., 1987; Heinricher et al., 1987; Ness and Gebhart, 1987; Carstens et al., 1988; Jacquet, 1988; Jones and Gebhart, 1988; Jensen and Yaksh, 1989; Siegfried and de Souza, 1989; Behbehani et al., 1990; Carstens et al., 1990). The magnitude of antinociceptive effects observed after global chemogenetic activation of vPAG neurons is modest relative to the robust effects produced by electrical stimulation of the PAG or by microinjection of morphine, GABA_A receptor antagonists, or glutamate agonists into the vPAG (Reynolds, 1969; Liebeskind et al., 1973; Moreau and Fields, 1986; Depaulis et al., 1987; Ness and Gebhart, 1987; Carstens et al., 1988; Sandkühler et al., 1989; Siegfried and de Souza, 1989; Carstens et al., 1990). Such a difference could be expected if the number of neurons that are transduced with stimulatory DREADDs

is small relative to the large number of neurons impacted by electrical or pharmacologic approaches.

Although the vIPAG has been extensively studied for its role in endogenous descending pain modulation (Reynolds, 1969; Liebeskind et al., 1973; Basbaum and Fields, 1978; Sandkühler et al., 1989; Behbehani et al., 1990; Vaughan et al., 1997; McGaraughty et al., 2003; Starowicz et al., 2007; Morgan et al., 2008; Waters and Lumb, 2008; Heinricher et al., 2009; Samineni et al., 2011; Wang et al., 2012; Ho et al., 2013; Lau and Vaughan, 2014; Tovote et al., 2016), previous studies have not yet determined how distinct subpopulations of vIPAG neurons modulate pain transmission. Inhibitory neurotransmission in the vIPAG is known to modulate nocifensive behaviors, since microinjecting a GABA agonist produces pronociceptive effects, while decreasing inhibitory neurotransmission by microinjection of GABA antagonists into the vIPAG produces antinociceptive effects to noxious stimuli (Moreau and Fields, 1986; Depaulis et al., 1987; Sandkühler et al., 1989; Budai and Fields, 1998; Morgan et al., 2003). Such studies led some to propose the vIPAG GABA disinhibition analgesia hypothesis (Basbaum and Fields, 1978; Fields, 2004). Corroborating this hypothesis, many studies have shown that mu opioid receptor agonists have direct inhibitory effects on GABAergic neurons of vIPAG. This causes analgesia when directly administered into the vIPAG, suggesting that inhibition of GABAergic vIPAG neuronal activity may be a major mechanism for opioid-induced analgesia (Chieng and Christie, 1996; Vaughan et al., 1997). The cellular mechanisms underlying the analgesic and hyperalgesic effects of manipulating inhibitory and excitatory neurotransmission in the vIPAG have not been directly evaluated (Moreau and Fields, 1986; Carstens et al., 1988; Jacquet, 1988; Sandkühler et al., 1989; Vaughan et al., 1997; Budai and Fields, 1998; Fields, 2004; Maione et al., 2006; Starowicz et al., 2007). It is not known how distinct neuron subpopulations in the vIPAG engage complex downstream circuits of the descending pain modulation pathway. For the first time, we show that chemogenetic activation of vIPAG GABAergic neurons causes hypersensitivity to nociceptive stimuli while their inhibition causes antinociception, consistent with the proposed role of GABAergic vIPAG neurons in pain modulation.

It has been hypothesized that GABAergic interneurons exert tonic inhibition of vIPAG glutamatergic neurons, which are thought to be output neurons that project to the RVM (Jacquet, 1988; Roychowdhury and Fields, 1996; Vaughan et al., 1997; Wang and Wessendorf, 2002; Morgan et al., 2008; Park et al., 2010; Hahm et al., 2011; Ho et al., 2013). These glutamatergic neurons have been hypothesized to play a role in an analgesic modulatory pathway (McGaraughty et al., 2003; Maione et al., 2006; Starowicz et al., 2007), but this has not been selectively demonstrated. In agreement with the GABA disinhibition hypothesis, our RNA-FISH studies show that GABAergic and glutamatergic neurons in the PAG are distinct populations. We also found that chemogenetic activation of vIPAG glutamatergic neurons is antinociceptive, whereas chemogenetic inhibition of these neurons is pronociceptive.

Conversely, chemogenetic activation of GABAergic neurons in the vIPAG produces hypersensitivity while inhibition of these neurons produces analgesia.

Surprisingly, we find that activation of vIPAG glutamatergic neurons or inhibition of GABAergic neurons attenuated thermal but not mechanical sensitivity. While there are several possible explanations for this finding, we propose the hypothesis that distinct populations of inhibitory neurons regulate mechanical and thermal nociceptive modulatory pathways emanating from the vIPAG. Here, we posit the presence of tonically active GABAergic neurons regulating descending pathways for thermal nociception, while the population regulating mechanical nociceptive modulation might be quiescent. This would explain the difference in effects of activating GABAergic neurons or inhibiting glutamatergic neurons on mechanical nociception. It is possible that the differences in the effects of DREADD-dependent regulation are simply due to the basal state of the neurons in question. That is, if the neurons are quiescent at baseline, then activation of a G_i -coupled DREADD might not affect descending modulation. Similarly, a neuron that is firing at a relatively high frequency at baseline might not be further stimulated by a G_q -coupled DREADD. Future studies are necessary to determine the differences in neuronal populations and circuits that code for mechanical versus thermal sensitivity. It is also possible that these results are simply due to a ceiling effect in our von Frey measurements. That is, that von Frey testing is not able to detect analgesic effects at baseline. We do not favor this hypothesis, as treatment with analgesic drugs can indeed increase PWTs in mice (Anseloni and Gold, 2008).

We believe that our results should not be interpreted as absolute, and we recognize that the behavioral changes that we report should not be attributed to the entirety of either the Vgat or Vglut2 vIPAG neuronal populations. The PAG is comprised of molecularly diverse neuronal subpopulations that express fast neurotransmitters and/or neuropeptides (Mantyh, 1982; Moss and Basbaum, 1983; Moss et al., 1983; Smith et al., 1994). In the hypothalamus, recent genetic analysis of anatomically defined neurons has identified subpopulations that coexpress a variety of neuroactive substances that were previously thought to be exclusive to certain clusters (Romanov et al., 2017). Therefore, it is likely that vIPAG GABAergic and glutamatergic neurons can be further subdivided into subpopulations based on their genetic identity and physiology. Although we have only attempted to dissect the roles of glutamatergic versus GABAergic vIPAG neurons in pain modulation, future studies should examine the interplay between other neuronal populations within the vIPAG that can be defined with the expression of other makers, such as neuropeptides, to assess their roles in regulating nociceptive processing.

While the stimulation of vIPAG is predominantly associated with antinociceptive effects (Reynolds, 1969; Liebeskind et al., 1973; Carstens et al., 1988; Morgan et al., 1989; Sandkühler et al., 1989; Hohmann et al., 2005; Maione et al., 2006; Starowicz et al., 2007; Samineni et al., 2011), recent studies also identified facilitatory effects of the vIPAG in

the maintenance of neuropathic pain (Pertovaara et al., 1996; Pertovaara et al., 1997; Heinricher et al., 2004; Guo et al., 2006; Lü et al., 2010). We show here that chemo-genetic activation of GABAergic neurons or inhibition of glutamatergic neurons can lead to hypersensitivity to mechanical and thermal stimuli, suggesting that any disruption of the balance between activity of the vIPAG excitatory and inhibitory neurons might contribute to the maintenance of chronic pain (Hahm et al., 2011; Ho et al., 2013; Lau and Vaughan, 2014). Future studies should explore the plastic changes in GABAergic and glutamatergic neurons that might contribute to the maintenance of chronic pain.

The vIPAG has been shown to be instrumental in the descending modulation of pain processing. The vIPAG is known to form strong connections with the RVM, and the locus coeruleus (Beitz et al., 1983; Behbehani, 1995; Antal and Odeh, 1998; Odeh and Antal, 2001; Bowman et al., 2013). Based on the data we present here, it will be of great interest to determine which of these, or other, projection targets mediate the differential modulation of nociception by glutamatergic and GABAergic projections from the vIPAG.

References

- Anseloni VC, Gold MS (2008) Inflammation-induced shift in the valence of spinal GABA-A receptor-mediated modulation of nociception in the adult rat. *J Pain* 9:732–738. [CrossRef](#)
- Antal M, Odeh F (1998) The projections of the midbrain periaqueductal gray to serotonergic and noradrenergic nuclei of the pons and medulla oblongata in the rat. *Eur J Neurosci* 10:218–218.
- Bandler R, Keay KA (1996) Columnar organization in the midbrain periaqueductal gray and the integration of emotional expression. *Prog Brain Res* 107:285–300. [Medline](#)
- Basbaum AI, Fields HL (1978) Endogenous pain control mechanisms: review and hypothesis. *Ann Neurol* 4:451–462. [CrossRef](#) [Medline](#)
- Basbaum AI, Fields HL (1979) The origin of descending pathways in the dorsolateral funiculus of the spinal cord of the cat and rat: further studies on the anatomy of pain modulation. *J Comp Neurol* 187:513–531. [CrossRef](#) [Medline](#)
- Baskin DS, Mehler WR, Hosobuchi Y, Richardson DE, Adams JE, Flitter MA (1986) Autopsy analysis of the safety, efficacy and cartography of electrical-stimulation of the central gray in humans. *Brain Res* 371:231–236. [Medline](#)
- Behbehani MM (1995) Functional characteristics of the midbrain periaqueductal gray. *Prog Neurobiol* 46:575–605. [Medline](#)
- Behbehani MM, Fields HL (1979) Evidence that an excitatory connection between the periaqueductal gray and nucleus raphe magnus mediates stimulation produced analgesia. *Brain Res* 170:85–93. [Medline](#)
- Behbehani MM, Jiang MR, Chandler SD, Ennis M (1990) The effect of GABA and its antagonists on midbrain periaqueductal gray neurons in the rat. *Pain* 40:195–204. [Medline](#)
- Beitz AJ, Mullett MA, Weiner LL (1983) The periaqueductal gray projections to the rat spinal trigeminal, raphe magnus, gigantocellular pars alpha and paragigantocellular nuclei arise from separate neurons. *Brain Res* 288:307–314. [Medline](#)
- Bennett GJ, Mayer DJ (1979) Inhibition of spinal cord interneurons by narcotic microinjection and focal electrical stimulation in the periaqueductal central gray matter. *Brain Res* 172:243–257. [Medline](#)
- Bowman BR, Kumar NN, Hassan SF, McMullan S, Goodchild AK (2013) Brain sources of inhibitory input to the rat rostral ventrolateral medulla. *J Comp Neurol* 521:213–232. [CrossRef](#) [Medline](#)
- Budai D, Fields HL (1998) Endogenous opioid peptides acting at mu-opioid receptors in the dorsal horn contribute to midbrain modulation of spinal nociceptive neurons. *J Neurophysiol* 79:677–687. [Medline](#)
- Carstens E, Hartung M, Stelzer B, Zimmermann M (1990) Suppression of a hind-limb flexion withdrawal reflex by microinjection of glutamate or morphine into the periaqueductal gray in the rat. *Pain* 43:105–112. [Medline](#)
- Carstens E, Stelzer B, Zimmermann M (1988) Microinjections of glutamate or morphine at coincident midbrain sites have different effects on nociceptive dorsal horn neurons in the rat. *Neurosci Lett* 95:185–191. [Medline](#)
- Chiang B, Christie MD (1996) Local opioid withdrawal in rat single periaqueductal gray neurons in vitro. *J Neurosci* 16:7128–7136. [Medline](#)
- Depaulis A, Morgan MM, Liebeskind JC (1987) Gabaergic modulation of the analgesic effects of morphine microinjected in the ventral periaqueductal gray-matter of the rat. *Brain Res* 436:223–228. [Medline](#)
- Duggan AW, Morton CR (1983) Periaqueductal grey stimulation: an association between selective inhibition of dorsal horn neurones and changes in peripheral circulation. *Pain* 15:237–248. [Medline](#)
- Fields H (2004) State-dependent opioid control of pain. *Nat Rev Neurosci* 5:565–575. [CrossRef](#) [Medline](#)
- Graeff FG, Silveira MC, Nogueira RL, Audi EA, Oliveira RM (1993) Role of the amygdala and periaqueductal gray in anxiety and panic. *Behav Brain Res* 58:123–131. [Medline](#)
- Guo W, Robbins MT, Wei F, Zou S, Dubner R, Ren K (2006) Supraspinal brain-derived neurotrophic factor signaling: a novel mechanism for descending pain facilitation. *J Neurosci* 26:126–137. [CrossRef](#) [Medline](#)
- Hahm ET, Kim Y, Lee JJ, Cho YW (2011) GABAergic synaptic response and its opioidergic modulation in periaqueductal gray neurons of rats with neuropathic pain. *BMC Neurosci* 12:41. [CrossRef](#) [Medline](#)
- Hayes RL, Price DD, Ruda M, Dubner R (1979) Suppression of nociceptive responses in the primate by electrical stimulation of the brain or morphine administration: behavioral and electrophysiological comparisons. *Brain Res* 167:417–421. [Medline](#)
- Heinricher MM, Cheng ZF, Fields HL (1987) Evidence for two classes of nociceptive modulating neurons in the periaqueductal gray. *J Neurosci* 7:271–278. [Medline](#)
- Heinricher MM, Martenson ME, Neubert MJ (2004) Prostaglandin E2 in the midbrain periaqueductal gray produces hyperalgesia and activates pain-modulating circuitry in the rostral ventromedial medulla. *Pain* 110:419–426. [CrossRef](#) [Medline](#)
- Heinricher MM, Tavares I, Leith JL, Lumb BM (2009) Descending control of nociception: specificity, recruitment and plasticity. *Brain Res Rev* 60:214–225. [CrossRef](#) [Medline](#)
- Ho YC, Cheng JK, Chiou LC (2013) Hypofunction of glutamatergic neurotransmission in the periaqueductal gray contributes to nerve-injury-induced neuropathic pain. *J Neurosci* 33:7825–7836. [CrossRef](#) [Medline](#)
- Hohmann AG, Suplita RL, Bolton NM, Neely MH, Fegley D, Mangieri R, Krey JF, Walker JM, Holmes PV, Crystal JD, Duranti A, Tontini A, Mor M, Tarzia G, Piomelli D (2005) An endocannabinoid mechanism for stress-induced analgesia. *Nature* 435:1108–1112. [CrossRef](#) [Medline](#)
- Holstege G (2014) The periaqueductal gray controls brainstem emotional motor systems including respiration. *Prog Brain Res* 209:379–405. [CrossRef](#) [Medline](#)
- Hosobuchi Y, Adams JE, Linchitz R (1977) Pain relief by electrical stimulation of the central gray matter in humans and its reversal by naloxone. *Science* 197:183–186. [Medline](#)
- Jacquet YF (1988) The Nmnda receptor - central role in pain inhibition in rat periaqueductal gray. *Eur J Pharmacol* 154:271–276. [Medline](#)
- Jensen TS, Yaksh TL (1989) Comparison of the antinociceptive effect of morphine and glutamate at coincidental sites in the periaqueductal gray and medial medulla in rats. *Brain Res* 476:1–9. [Medline](#)

- Jones SL, Gebhart GF (1988) Inhibition of spinal nociceptive transmission from the midbrain, pons and medulla in the rat - activation of descending inhibition by morphine, glutamate and electrical stimulation. *Brain Res* 460:281–296. [Medline](#)
- Lau BK, Vaughan CW (2014) Descending modulation of pain: the GABA disinhibition hypothesis of analgesia. *Curr Opin Neurobiol* 29:159–164. [CrossRef](#) [Medline](#)
- Liebeskind JC, Guilbaud G, Besson JM, Oliveras JL (1973) Analgesia from electrical stimulation of the periaqueductal gray matter in the cat: behavioral observations and inhibitory effects on spinal cord interneurons. *Brain Res* 50:441–446. [Medline](#)
- Lü N, Han M, Yang ZL, Wang YQ, Wu GC, Zhang YQ (2010) Nociceptin/orphanin FQ in PAG modulates the release of amino acids, serotonin and norepinephrine in the rostral ventromedial medulla and spinal cord in rats. *Pain* 148:414–425. [CrossRef](#) [Medline](#)
- Maione S, Bisogno T, de Novellis V, Palazzo E, Cristino L, Valenti M, Petrosino S, Guglielmotti V, Rossi F, Di Marzo V (2006) Elevation of endocannabinoid levels in the ventrolateral periaqueductal grey through inhibition of fatty acid amide hydrolase affects descending nociceptive pathways via both cannabinoid receptor type 1 and transient receptor potential vanilloid type-1 receptors. *J Pharmacol Exp Ther* 316:969–982. [CrossRef](#) [Medline](#)
- Mantyh PW (1982) The midbrain periaqueductal gray in the rat, cat, and monkey: a Nissl, Weil, and Golgi analysis. *J Comp Neur* 204:349–363. [CrossRef](#) [Medline](#)
- Mayer DJ, Liebeskind JC (1974) Pain reduction by focal electrical stimulation of the brain: an anatomical and behavioral analysis. *Brain Res* 68:73–93. [Medline](#)
- McGarraughy S, Chu KL, Bitner RS, Martino B, El Kouhen R, Han P, Nikkel AL, Burgard EC, Faltynek CR, Jarvis MF (2003) Capsaicin infused into the PAG affects rat tail flick responses to noxious heat and alters neuronal firing in the RVM. *J Neurophysiol* 90:2702–2710. [CrossRef](#) [Medline](#)
- Millan MJ, Członkowski A, Millan MH, Herz A (1987) Activation of periaqueductal grey pools of beta-endorphin by analgetic electrical stimulation in freely moving rats. *Brain Res* 407:199–203. [Medline](#)
- Moreau JL, Fields HL (1986) Evidence for GABA involvement in midbrain control of medullary neurons that modulate nociceptive transmission. *Brain Res* 397:37–46. [Medline](#)
- Morgan MM, Clayton CC, Lane DA (2003) Behavioral evidence linking opioid-sensitive GABAergic neurons in the ventrolateral periaqueductal gray to morphine tolerance. *Neuroscience* 118:227–232. [Medline](#)
- Morgan MM, Sohn JH, Liebeskind JC (1989) Stimulation of the periaqueductal gray-matter inhibits nociception at the supraspinal as well as spinal level. *Brain Res* 502:61–66. [Medline](#)
- Morgan MM, Whittier KL, Hegarty DM, Aicher SA (2008) Periaqueductal gray neurons project to spinally projecting GABAergic neurons in the rostral ventromedial medulla. *Pain* 140:376–386. [CrossRef](#) [Medline](#)
- Morton CR, Duggan AW, Zhao ZQ (1984) The effects of lesions of medullary midline and lateral reticular areas on inhibition in the dorsal horn produced by periaqueductal grey stimulation in the cat. *Brain Res* 301:121–130. [Medline](#)
- Moss MS, Basbaum AI (1983) The peptidergic organization of the cat periaqueductal gray. II. The distribution of immunoreactive substance P and vasoactive intestinal polypeptide. *J Neurosci* 3:1437–1449. [Medline](#)
- Moss MS, Glazer EJ, Basbaum AI (1983) The peptidergic organization of the cat periaqueductal gray. I. The distribution of immunoreactive enkephalin-containing neurons and terminals. *J Neurosci* 3:603–616. [Medline](#)
- Ness TJ, Gebhart GF (1987) Quantitative comparison of inhibition of visceral and cutaneous spinal nociceptive transmission from the midbrain and medulla in the rat. *J Neurophysiol* 58:850–865. [Medline](#)
- O'Brien DE, Brenner DS, Gutmann DH, Gereau RW (2013) Assessment of pain and itch behavior in a mouse model of neurofibromatosis type 1. *J Pain* 14:628–637.
- Odeh F, Antal M (2001) The projections of the midbrain periaqueductal grey to the pons and medulla oblongata in rats. *Eur J Neurosci* 14:1275–1286. [Medline](#)
- Park C, Kim JH, Yoon BE, Choi EJ, Lee CJ, Shin HS (2010) T-type channels control the opioidergic descending analgesia at the low threshold-spiking GABAergic neurons in the periaqueductal gray. *Proc Natl Acad Sci USA* 107:14857–14862. [CrossRef](#) [Medline](#)
- Pertovaara A, Kontinen VK, Kalso EA (1997) Chronic spinal nerve ligation induces changes in response characteristics of nociceptive spinal dorsal horn neurons and in their descending regulation originating in the periaqueductal gray in the rat. *Exp Neurol* 147:428–436. [CrossRef](#) [Medline](#)
- Pertovaara A, Wei H, Hämäläinen MM (1996) Lidocaine in the rostral ventromedial medulla and the periaqueductal gray attenuates allodynia in neuropathic rats. *Neurosci Lett* 218:127–130. [Medline](#)
- Reichling DB, Basbaum AI (1990a) Contribution of brainstem GABAergic circuitry to descending antinociceptive controls: II. Electron microscopic immunocytochemical evidence of GABAergic control over the projection from the periaqueductal gray to the nucleus raphe magnus in the rat. *J Comp Neur* 302:378–393.
- Reichling DB, Basbaum AI (1990b) Contribution of brainstem GABAergic circuitry to descending antinociceptive controls: I. GABA-immunoreactive projection neurons in the periaqueductal gray and nucleus raphe magnus. *J Comp Neur* 302:370–377.
- Reynolds DV (1969) Surgery in the rat during electrical analgesia induced by focal brain stimulation. *Science* 164:444–445. [Medline](#)
- Rogan SC, Roth BL (2011) Remote control of neuronal signaling. *Pharmacol Rev* 63:291–315. [CrossRef](#) [Medline](#)
- Romanov RA, Zeisel A, Bakker J, Girach F, Hellysaz A, Tomer R, Alpár A5,6, Mulder J7, Clotman F8, Keimpema E1, Hsueh B4, Crow AK4, Martens H9, Schwindling C10, Calvigioni D1,3, Bains JS11, Máté Z12, Szabó G12, Yanagawa Y13, Zhang MD, et al. (2017) Molecular interrogation of hypothalamic organization reveals distinct dopamine neuronal subtypes. *Nat Neurosci* 20:176–188. [CrossRef](#) [Medline](#)
- Roychowdhury SM, Fields HL (1996) Endogenous opioids acting at a medullary mu-opioid receptor contribute to the behavioral antinociception produced by GABA antagonism in the midbrain periaqueductal gray. *Neuroscience* 74:863–872. [CrossRef](#)
- Samineni VK, Premkumar LS, Faingold CL (2011) Post-ictal analgesia in genetically epilepsy-prone rats is induced by audiogenic seizures and involves cannabinoid receptors in the periaqueductal gray. *Brain Res* 1389:177–182. [CrossRef](#) [Medline](#)
- Sandkühler J, Willmann E, Fu QG (1989) Blockade of GABA receptors in the midbrain periaqueductal gray abolishes nociceptive spinal dorsal horn neuronal-activity. *Eur J Pharmacol* 160:163–166. [Medline](#)
- Siegfried B, de Souza RL (1989) NMDA receptor blockade in the periaqueductal grey prevents stress-induced analgesia in attacked mice. *Eur J Pharmacol* 168:239–242. [Medline](#)
- Siuda ER, Copits BA, Schmidt MJ, Baird MA, Al-Hasani R, Planer WJ, Funderburk SC, McCall JG, Gereau RWt, Bruchas MR (2015) Spatiotemporal control of opioid signaling and behavior. *Neuron* 86:923–935. [CrossRef](#)
- Smith GS, Savery D, Marden C, López Costa JJ, Averill S, Priestley JV, Rattray M (1994) Distribution of messenger RNAs encoding enkephalin, substance P, somatostatin, galanin, vasoactive intestinal polypeptide, neuropeptide Y, and calcitonin gene-related peptide in the midbrain periaqueductal grey in the rat. *J Comp Neur* 350:23–40. [CrossRef](#)
- Starowicz K, Maione S, Cristino L, Palazzo E, Marabese I, Rossi F, de Novellis V, Di Marzo V (2007) Tonic endovanilloid facilitation of glutamate release in brainstem descending antinociceptive pathways. *J Neurosci* 27:13739–13749. [CrossRef](#) [Medline](#)
- Sternson SM, Roth BL (2014) Chemogenetic tools to interrogate brain functions. *Annu Rev Neurosci* 37:387–407. [CrossRef](#) [Medline](#)
- Tovote P, Esposito MS, Botta P, Haudun FC, Fadok JP, Markovic M, Wolff SBE, Ramakrishnan C, Fenno L, Deisseroth K, Herry C, Arber S, Luthi A (2016) Midbrain circuits for defensive behaviour. *Nature* 534:206–212.

- Urban DJ, Roth BL (2015) DREADDs (designer receptors exclusively activated by designer drugs): chemogenetic tools with therapeutic utility. *Annu Rev Pharmacol Toxicol* 55:399–417. [CrossRef](#) [Medline](#)
- Urban MO, Smith DJ (1994) Localization of the antinociceptive and antianalgesic effects of neurotensin within the rostral ventromedial medulla. *Neurosci Lett* 174:21–25. [Medline](#)
- Vaughan CW, Ingram SL, Connor MA, Christie MJ (1997) How opioids inhibit GABA-mediated neurotransmission. *Nature* 390:611–614. [CrossRef](#) [Medline](#)
- Vong L, Ye CP, Yang ZF, Choi B, Chua S, Lowell BB (2011) Leptin action on GABAergic neurons prevents obesity and reduces inhibitory tone to POMC neurons. *Neuron* 71:142–154. [CrossRef](#)
- Wang F, Flanagan J, Su N, Wang LC, Bui S, Nielson A, Wu X, Vo HT, Ma XJ, Luo Y (2012) RNAscope: a novel in situ RNA analysis platform for formalin-fixed, paraffin-embedded tissues. *J Mol Diagn* 14:22–29. [CrossRef](#) [Medline](#)
- Wang H, Wessendorf MW (2002) Mu- and delta-opioid receptor mRNAs are expressed in periaqueductal gray neurons projecting to the rostral ventromedial medulla. *Neuroscience* 109:619–634. [Medline](#)
- Waters AJ, Lumb BM (1997) Inhibitory effects evoked from both the lateral and ventrolateral periaqueductal grey are selective for the nociceptive responses of rat dorsal horn neurones. *Brain Res* 752:239–249. [Medline](#)
- Waters AJ, Lumb BM (2008) Descending control of spinal nociception from the periaqueductal grey distinguishes between neurons with and without C-fibre inputs. *Pain* 134:32–40. [CrossRef](#) [Medline](#)
- Watkins LR, Young EG, Kinscheck IB, Mayer DJ (1983) The neural basis of footshock analgesia: the role of specific ventral medullary nuclei. *Brain Res* 276:305–315. [Medline](#)
- Watson TC, Cerminara NL, Lumb BM, Apps R (2016) Neural correlates of fear in the periaqueductal gray. *J Neurosci* 36:12707–12719. [CrossRef](#) [Medline](#)
- Yeung JC, Yaksh TL, Rudy TA (1977) Concurrent mapping of brain sites for sensitivity to the direct application of morphine and focal electrical stimulation in the production of antinociception in the rat. *Pain* 4:23–40. [Medline](#)